MIT Libraries | DSpace@MIT

MIT Open Access Articles

Graphene Oxide Nanosheets Modified with Single-Domain Antibodies for Rapid and Efficient Capture of Cells

The MIT Faculty has made this article openly available. ***Please share*** how this access benefits you. Your story matters.

Citation: Chen, Guan-Yu et al. "Graphene Oxide Nanosheets Modified with Single-Domain Antibodies for Rapid and Efficient Capture of Cells." Chemistry - A European Journal 21.48 (2015): 17178–17183.

As Published: http://dx.doi.org/10.1002/chem.201503057

Publisher: Wiley Blackwell

Persistent URL: http://hdl.handle.net/1721.1/106212

Version: Author's final manuscript: final author's manuscript post peer review, without publisher's formatting or copy editing

Terms of use: Creative Commons Attribution-Noncommercial-Share Alike

Massachusetts Institute of Technology

Author Manuscript

Author Manuscript

Author Manuscript

Author Manuscript

HHS Public Access

Author manuscript

Chemistry. Author manuscript; available in PMC 2016 November 23.

Published in final edited form as:

Chemistry. 2015 November 23; 21(48): 17178–17183. doi:10.1002/chem.201503057.

Graphene Oxide Nanosheets Modified with Single Domain Antibodies for Rapid and Efficient Capture of Cells**

Guan-Yu Chen[+],
Whitehead Institute for Biomedical Research, Cambridge, MA 02142, USA

Zeyang Li[+],
Whitehead Institute for Biomedical Research, Cambridge, MA 02142, USA

Christopher S. Theile,
Whitehead Institute for Biomedical Research, Cambridge, MA 02142, USA

Neelkanth M. Bardhan,
Department of Materials Science and Engineering, The David H. Koch Institute for Integrative Cancer Research, Massachusetts Institute of Technology, Cambridge, MA 02139, USA

Priyank V. Kumar,
Department of Materials Science and Engineering, Massachusetts Institute of Technology, Cambridge, MA 02139, USA

Joao N. Duarte,
Whitehead Institute for Biomedical Research, Cambridge, MA 02142, USA

Takeshi Maruyama,
Whitehead Institute for Biomedical Research, Cambridge, MA 02142, USA

Ali Rashidfarrokh,
Whitehead Institute for Biomedical Research, Cambridge, MA 02142, USA

Angela M. Belcher, and
Department of Materials Science and Engineering, Department of Biological Engineering, The David H. Koch Institute for Integrative Cancer Research, Massachusetts Institute of Technology, Cambridge, MA 02139, USA

Hidde L. Ploegh
Department of Biology, Whitehead Institute for Biomedical Research, Massachusetts Institute of Technology, Cambridge, MA 02142, USA

Hidde L. Ploegh: ploegh@wi.mit.edu

Abstract

**The authors acknowledge the financial support from the National Science Council, Taiwan (NSC 102-2917-I-564-001-A1), Calouste Gulbenkian Foundation, Portuguese Science and Technology Foundation, Champalimaud Foundation and the National Institutes of Health. Supporting information for this article is given via a link at the end of the document.

Correspondence to: Hidde L. Ploegh, ploegh@wi.mit.edu.

Present address: G.-Y. Chen, Institute of Biomedical Engineering, National Chiao Tung University, Hsinchu 30010, Taiwan
[+]These authors contributed equally to this work

Author Manuscript Author Manuscript Author Manuscript Author Manuscript

Peripheral blood can provide valuable information on an individual's immune status. Cell-based assays typically target leukocytes and their products. Characterization of leukocytes from whole blood requires their separation from the far more numerous red blood cells.[1] Current methods to classify leukocytes, such as recovery on antibody-coated beads or fluorescence-activated cell sorting require long sample preparation times and relatively large sample volumes.[2] A simple method that enables the characterization of cells from a small peripheral whole blood sample could overcome limitations of current analytical techniques. We describe the development of a simple graphene oxide surface coated with single domain antibody fragments. This format allows quick and efficient capture of distinct WBC subpopulations from small samples (~30 μL) of whole blood in a geometry that does not require any specialized equipment such as cell sorters or microfluidic devices.

Keywords

single domain antibody; graphene oxide; sortase; blood; cell detection

Graphene oxide (GO) is a derivative of graphene, which can be modified for various applications, including bioassays,[3] bioimaging[4] and biosensors to select for different cell types.[5] The biocompatibility of GO offers many features attractive for optical biosensing platforms, such as a large surface area, good water dispersibility, and ease of facial surface modification. Full-sized antibodies can be attached to GO to create biosensors for the capture of circulating tumor cells from blood samples and for virus detection.[5–6] However, the full sized antibody-GO platform has several drawbacks that prevent it from being used for high throughput screening. Full-sized antibodies are costly and not always easy to produce. Construction of the circulating tumor cell-antibody-GO biosensor requires special equipment to produce the necessary GO-gold surface[5]. Furthermore, antibodies are usually coupled to the GO surface via NHS ester or maleimide chemistries, which target free lysine or cysteine residues respectively, with possible loss of activity.[6–7] The use of NHS-lysine and maleimide-cysteine coupling complicates further functionalization of the antibody. For example, free lysine and cysteines not involved in covalent attachment to the GO surface could be functionalized with dyes, but attaining quantitative and homogeneous labeling would be challenging. Attaching antibodies through biotin-streptavidin/NeutrAvidin interactions introduces additional complexity and usually relies on biotinylation strategies that –again- involve lysine or cysteine modifications.[5, 8]

We address these limitations by attaching single domain antigen-binding fragments derived from camelid heavy-chain-only antibodies, known as VHHs or nanobodies,[9] directly to the GO surface in a site-specific manner using sortase. VHHs are small (~15 KDa) and are easily expressed in bacteria; they are monomeric and have an excellent thermo-chemical stability profile, all of which make them suitable for diagnostic and therapeutic applications.[10] A sizable portion of the VHH's surface is involved in binding interactions, and therefore site-specific modifications of a VHH at a position distal form the antigen binding site is essential to obtain a properly oriented coating, a prerequisite to build an efficient biosensor.[7, 11] We used a combination of a sortase-mediated transpeptidation reaction in combination with 'click' chemistry to site-specifically attach a fluorescently

Author Manuscript Author Manuscript Author Manuscript Author Manuscript

labeled VHH via a carboxyterminal LPXTG motif to PEG linker-modified GO.[11–12] We thus installed an anti-murine Class II MHC VHH (VHH7)[13] and an anti-murine CD11b VHH (VHH DC13), both sortase-labeled with a TAMRA fluorophore, to GO nanosheets. The combination of these functionalized surfaces allowed us to selectively capture Class II MHC-positive (MHC^+) and CD11b-positive ($CD11b^+$) cells from small volumes (~30 μL) of peripheral blood (Fig. 1) with minimal handling in a device of simple geometry.

GO nanosheets (<2 nm thickness, 500 nm mean diameter) functionalized with carboxylic acids were dispersed in deionized water. For the preparation of nanosubstrates, GO was immobilized on a 3-aminopropyltriethoxysilane (APTES)- functionized glass slide by means of electrostatic forces between the oxide groups of GO and the amine-end of 3-APTES.[14] Scanning electron microscopy (SEM) images of GO nanosheets immobilized on a silicon substrate showed even and dense coverage of thin sheets on the surface, with spacing between adjacent sheets < 2 μm (Fig. S1). The GO nanosheets were covalently functionalized with diamino-functionalized polyethylene glycol (NH_2-$(PEG)_n$-NH_2) (Fig. S2). The presence of epoxide, hydroxyl, carbonyl, carboxyl and amine groups was confirmed by X-ray photoelectron spectroscopy (XPS) (Fig. S3). Dibenzocyclooctyne-N-hydroxysuccinimidyl ester (DBCO-NHS) was then reacted with the terminal amines of the PEG chains to install a ‘click’ chemistry handle onto the GO surface (Fig. S2).

To assess the potential of GO-immobilized VHH for cell capture, we first engineered a sortase-ready version of VHH7 with an LPETG motif near the C-terminus.[13] Using standard sortagging protocols[13] we introduced a Gly_3 peptide equipped with a TAMRA fluorophore and an azide, to partner with the DBCO moiety during the ‘click’ reaction. We included the TAMRA fluorophore to create fluorescence microscopy overlays between the VHH-GO surface and a fluorescently stained cell (Fig. S4). Thus modified VHH7 was covalently coupled in a uniform orientation onto a GO nanosheet upon reaction of the DBCO and azide groups in a cycloaddition (Fig. 2a). Atomic force microscopy (AFM) images showed that the VHH7-immobilized GO nanosheets exhibited a clear difference in height profile with a vertical size ranging from 20 to 80 nm (Fig. 2b), attributable to immobilization of VHH7 on the nanosheets.

The VHH7-GO functionalized slide was assembled with a second glass slide to form a cell capture chamber. Two strips of double-sided tape served as spacers to yield a chamber of approximately 12 mm × 25 mm × ~0.1 mm for a total volume of ~30 μL. The VHH is thus directly attached to one of the surfaces of the capture chamber. Assembly of this device requires no more than two-sided tape and a second, unmodified glass slide (Fig. 2c). Delivery of ~30 μL of whole blood or a cell suspension is then achieved by contacting the opening of the chamber with the tip of a mechanical pipetting device. Within seconds, discharge of the intended volume then fills the chamber by capillary action. Wash steps are conducted in similar fashion by delivery of buffer to one open side of the chamber, and wicking off buffer at the opposite end of the chamber, using filter paper to ensure flow across the chamber surfaces.

To verify the specificity of GO-immobilized VHH7 for murine Class II MHC^+ cells, mouse B lymphoma (A20) and human B lymphoma (Raji, murine Class II MHC-negative) cell

Author Manuscript Author Manuscript Author Manuscript Author Manuscript

lines were labeled with a fluorescent cell tracker dye, diluted in PBS and loaded into the VHH-GO device for 10 min at 37°C. Different cell densities were applied to optimize loading conditions (Fig. 3a, b). When ~2.2×10^4 A20 cells were seeded, ~83% of the cells were captured. As the number of loaded cells increased to 6–7×10^4, approximately half of the cells were retained. There was little difference when the number of cells loaded was increased to ~20×10^4, as just ~4.3×10^4 were captured. For A20 cells, the functionalized nanosubstrate showed a capture yield of A20 cells of ~80 % for ~2.2×10^4 loaded cells, compared to ~17 % for an unmodified GO surface (Fig. 3c). Human Raji cells showed no significant difference in binding to the VHH7-functionalized (~21%) and the unmodified GO surface (~15%), demonstrating the specificity of VHH7 for its target (Fig. 3d). GO nanosheets modified with VHH7 thus efficiently captured murine Class II MHC$^+$ cells (Fig. 3e and Fig. S5).

We next tested performance of the VHH7-modified nanosubstrate on whole blood. Fresh blood was obtained from Class II MHC-eGFP knock-in mice for ready visualization of Class II MHC$^+$ cells by their GFP fluorescence (Fig. S6). Analysis of Class II MHC-eGFP$^+$ cells showed an average capture efficiency of ~74 % (n=5) on the VHH7-functionalized nanosubstrate (~11,000 cells). Conversely, without VHH7, only ~14 % of eGFP$^+$ cells (~2,000 cells) were retained (Fig. 4a, b and Table S1), in agreement with what was observed with the A20 cell line. A similarly low capture yield (~11%) was seen when using an irrelevant VHH for immobilization (Fig. S7). We saw co-localization of the Class II MHC-eGFP signal with the VHH7-TAMRA signal (Fig. 4c, d). When we counterstained VHH7-immobilized cells with Alexa647-labeled VHH7 and DAPI, we observed excellent colocalization of Alexa647-labeled VHH7 with Class II MHC-eGFP, showing that GO-VHH7 immobilized cells remained available for further staining *in situ* (Fig. 4e), with only minimal consumption of labeled antibody owing to the small volume of the chamber (~30 μL). Most eGFP$^+$ captured cells ranged from 10–15 μm in diameter, the size of B cells (Fig 4c). The identity of this population was further confirmed with Alexa647-labeled anti-IgG antibody for surface staining of B cell receptors (BCRs) (Fig. S8). B cells captured from OB-1-Class II MHC eGFP mice, which possess a BCR specific for ovalbumin[15] and its fragments retained the ability to bind and internalize an Alexa647-labeled ovalbumin fragment, the FGD-17mer peptide,[15–16] which ultimately colocalized with Class II-MHC-eGFP$^+$ compartments (Fig. S9).

To calculate the fraction of Class II MHC-negative cells bound to the VHH7-GO nanosubstrate, we disassembled the chamber after cell capture and stained captured cells using Alexa647-labeled anti CD45 (a surface marker for leukocytes) or Alexa647- labeled anti CD3 (a surface marker for T cells). After image acquisition, we used the merged information to identify Class II MHC-eGFP$^+$ cells, as shown in Fig. S10a, b. Confocal microscopy showed that all cells captured were CD45$^+$. Class II MHC-eGFP$^+$ cells comprised the majority (~76%), of captured cells, CD3$^+$ cells constitute up to ~21%, and the remaining leukocyte population is ~3% of the total (Fig. S10c). This observation is consistent with earlier observations that the captured cells from whole blood often contain non-specifically bound leukocytes.[17]

Author Manuscript Author Manuscript Author Manuscript Author Manuscript

To further demonstrate the utility of our method, we immobilized VHH DC13, specific for murine CD11b$^+$, onto a GO substrate, to capture other leukocytes. We analyzed the capture efficiency of GO-immobilized VHH DC13 alone and in conjunction with VHH7-GO. Capture efficiency and yield were similar to those observed for VHH7-Class II MHC$^+$ B-cells. Confocal microscopy showed that the majority of captured cells are CD11b$^+$ with fewer Class II MHC-eGFP$^+$ cells and CD11b/Class II MHC-eGFP double positive cells (Fig. S11)

To improve recovery of CD11b$^+$ populations, we created a capture chamber that allows the sample to pass sequentially over two surfaces, functionalized with VHH7 and VHH DC13 respectively (Fig. 5a, Fig. S12). Blood obtained from Class II MHC-eGFP knock-in mice was exposed first to the VHH7-modified substrate for 10 min, followed by flushing with PBS to transfer the sample onto the adjacent VHH DC13-modified substrate, where incubation continued for another 10 min. Captured cells were counterstained with Alexa647-labeled CD11b and DAPI and visualized by confocal microscopy. CD11b$^+$ cells (which are Class II MHC-eGFP negative cells) comprised the majority of captured cells on the VHH DC13-modified substrate (Fig 5b). Compared with cells directly captured on a VHH DC13-modified surface (Fig. S11), the combination of VHH7 and VHH DC13 significantly improves capture of CD11b$^+$ cells (95% instead of 66% of the VHH DC13 alone; Fig. 5c). Overall CD11b$^+$ cell capture yield (~3,500 cells) in the tandem array showed no loss compared to a surface functionalized with only VHH DC13 (Fig. 5d)

CD11b$^+$ cells captured on VHH DC13-modified substrates contain a bi- or multilobed nucleus characteristic of neutrophils (Fig. 5b).[18] The identity of this population was confirmed by surface staining with Alexa647-labeled anti Gr-1 (a surface marker for neutrophils) (Fig. S13). Neutrophils are part of the first line of defense against fungal pathogens such as *Candida albicans*, using their dectin-1 receptor to effectivate phagocytosis of *Candida albicans*.[18–19] The dually functionalized VHH7-VHH DC13 GO surface successfully captured CD11b$^+$ cells in the process of phagocytosing *Candida albicans* in the blood (Fig. 5e, Fig. S14). Confocal microscopy shows that during phagocytosis of *Candida albicans*, cell morphology changes (compare 30 and 60 min timepoints). A common limitation of working with primary neutrophils is their short lifespan.[18] Processing times required to isolate neutrophils by other methods, usually several hours, may alter their responsiveness compared to their behavior *in vivo*.[20] CD11b$^+$ cells can be rapidly captured (~20 min) in good yield (~95%) by dually functionalized VHH-modified substrates, thus providing rapid access to pure immobilized neutrophils with detection of phagocytic function.

Sortase conjugation of VHH7 in a uniform orientation onto GO nanosubstrates allows efficient capture of Class II MHC$^+$ cells from small amounts of blood. We generated a simple flow system for cells to pass successively over two surfaces, functionalized with VHH7 and VHH DC13 respectively, a configuration that increases the capture percentage of CD11b$^+$ cells. Sortase conjugation also allows site-specific and quantitative installation of additional fluorophores for co-localization microscopy with a fluorescent or fluorescently stained cells. This VHH-based sensing system is compatible with small blood or reagent sample volumes, rapid processing, stability, ease of manufacture and low cost. Stability of

Author Manuscript Author Manuscript Author Manuscript Author Manuscript

GO-VHH adducts might even eliminate the need for a cold chain and thus enable use of devices of this type outside the setting of the laboratory. Our method can easily be extended to other VHH's or biologicals for isolation, identification and analysis of other cell types in a minimally invasive approach.

Supplementary Material

Refer to Web version on PubMed Central for supplementary material.

Acknowledgments

The authors acknowledge the financial support from the Ministry of Science and Technology, Taiwan (MOST 104-2314-B-009-001-), Calouste Gulbenkian Foundation, Portuguese Science and Technology Foundation, Champalimaud Foundation and the National Institutes of Health. This study was supported in part by the Institute for Collaborative Biotechnologies through grant W911NF-09-0001 from the US Army Research Office. P.V.K. wishes to thank financial support from the Tata Center and Eni Solar Frontiers Program at MIT.

References

1. Sethu P, Moldawer LL, Mindrinos MN, Scumpia PO, Tannahill CL, Wilhelmy J, Efron PA, Brownstein BH, Tompkins RG, Toner M. Anal Chem. 2006; 78:5453–5461. [PubMed: 16878882]
2. a Li Y, Kurlander RJ. J Transl Med. 2010; 8:104. [PubMed: 20977748] b Zhang X, Goncalves R, Mosser DM. Curr Protoc Immunol. 2008 Chapter 14, Unit 14 11.
3. Mei Q, Zhang Z. Angew Chem Int Ed Engl. 2012; 51:5602–5606. [PubMed: 22539356]
4. Sreejith S, Ma X, Zhao Y. J Am Chem Soc. 2012; 134:17346–17349. [PubMed: 22799451]
5. Yoon HJ, Kim TH, Zhang Z, Azizi E, Pham TM, Paoletti C, Lin J, Ramnath N, Wicha MS, Hayes DF, Simeone DM, Nagrath S. Nat Nanotechnol. 2013; 8:735–741. [PubMed: 24077027]
6. Jung JH, Cheon DS, Liu F, Lee KB, Seo TS. Angew Chem Int Ed Engl. 2010; 49:5708–5711. [PubMed: 20602383]
7. Trilling AK, Harmsen MM, Ruigrok VJ, Zuilhof H, Beekwilder J. Biosens Bioelectron. 2013; 40:219–226. [PubMed: 22878083]
8. a Jeon S, Moon JM, Lee ES, Kim YH, Cho Y. Angew Chem Int Ed Engl. 2014; 53:4597–4602. [PubMed: 24652762] b Hou S, Zhao H, Zhao L, Shen Q, Wei KS, Suh DY, Nakao A, Garcia MA, Song M, Lee T, Xiong B, Luo SC, Tseng HR, Yu HH. Adv Mater. 2013; 25:1547–1551. [PubMed: 23255101]
9. a Muyldermans S. Annu Rev Biochem. 2013; 82:775–797. [PubMed: 23495938] b Holliger P, Hudson PJ. Nat Biotechnol. 2005; 23:1126–1136. [PubMed: 16151406] c Harmsen MM, De Haard HJ. Appl Microbiol Biotechnol. 2007; 77:13–22. [PubMed: 17704915]
10. De Meyer T, Muyldermans S, Depicker A. Trends Biotechnol. 2014; 32:263–270. [PubMed: 24698358]
11. Trilling AK, Hesselink T, van Houwelingen A, Cordewener JH, Jongsma MA, Schoffelen S, van Hest JC, Zuilhof H, Beekwilder J. Biosens Bioelectron. 2014; 60:130–136. [PubMed: 24793095]
12. a Mao H, Hart SA, Schink A, Pollok BA. J Am Chem Soc. 2004; 126:2670–2671. [PubMed: 14995162] b Ton-That H, Mazmanian SK, Faull KF, Schneewind O. J Biol Chem. 2000; 275:9876–9881. [PubMed: 10734144]
13. Witte MD, Cragnolini JJ, Dougan SK, Yoder NC, Popp MW, Ploegh HL. Proceedings of the National Academy of Sciences of the United States of America. 2012; 109:11993–11998. [PubMed: 22778432]
14. Chen GY, Pang DW, Hwang SM, Tuan HY, Hu YC. Biomaterials. 2012; 33:418–427. [PubMed: 22014460]
15. Dougan SK, Ogata S, Hu CC, Grotenbreg GM, Guillen E, Jaenisch R, Ploegh HL. Proceedings of the National Academy of Sciences of the United States of America. 2012; 109:13739–13744. [PubMed: 22869725]

Author Manuscript Author Manuscript Author Manuscript Author Manuscript

16. Avalos AM, Bilate AM, Witte MD, Tai AK, He J, Frushicheva MP, Thill PD, Meyer-Wentrup F, Theile CS, Chakraborty AK, Zhuang X, Ploegh HL. J Exp Med. 2014; 211:365–379. [PubMed: 24493799]

17. a Zhao L, Lu YT, Li F, Wu K, Hou S, Yu J, Shen Q, Wu D, Song M, Ouyang WH, Luo Z, Lee T, Fang X, Shao C, Xu X, Garcia MA, Chung LW, Rettig M, Tseng HR, Posadas EM. Adv Mater. 2013b Shen Q, Xu L, Zhao L, Wu D, Fan Y, Zhou Y, Ouyang WH, Xu X, Zhang Z, Song M, Lee T, Garcia MA, Xiong B, Hou S, Tseng HR, Fang X. Adv Mater. 2013; 25:2368–2373. [PubMed: 23495071]

18. a Branzk N, Lubojemska A, Hardison SE, Wang Q, Gutierrez MG, Brown GD, Papayannopoulos V. Nature immunology. 2014; 15:1017–1025. [PubMed: 25217981] b Kolaczkowska E, Kubes P. Nature reviews Immunology. 2013; 13:159–175.

19. a Strijbis K, Tafesse FG, Fairn GD, Witte MD, Dougan SK, Watson N, Spooner E, Esteban A, Vyas VK, Fink GR, Grinstein S, Ploegh HL. PLoS pathogens. 2013; 9:e1003446. [PubMed: 23825946] b Esteban A, Popp MW, Vyas VK, Strijbis K, Ploegh HL, Fink GR. Proceedings of the National Academy of Sciences of the United States of America. 2011; 108:14270–14275. [PubMed: 21825168]

20. Agrawal N, Toner M, Irimia D. Lab on a chip. 2008; 8:2054–2061. [PubMed: 19023468]

Author Manuscript Author Manuscript Author Manuscript Author Manuscript

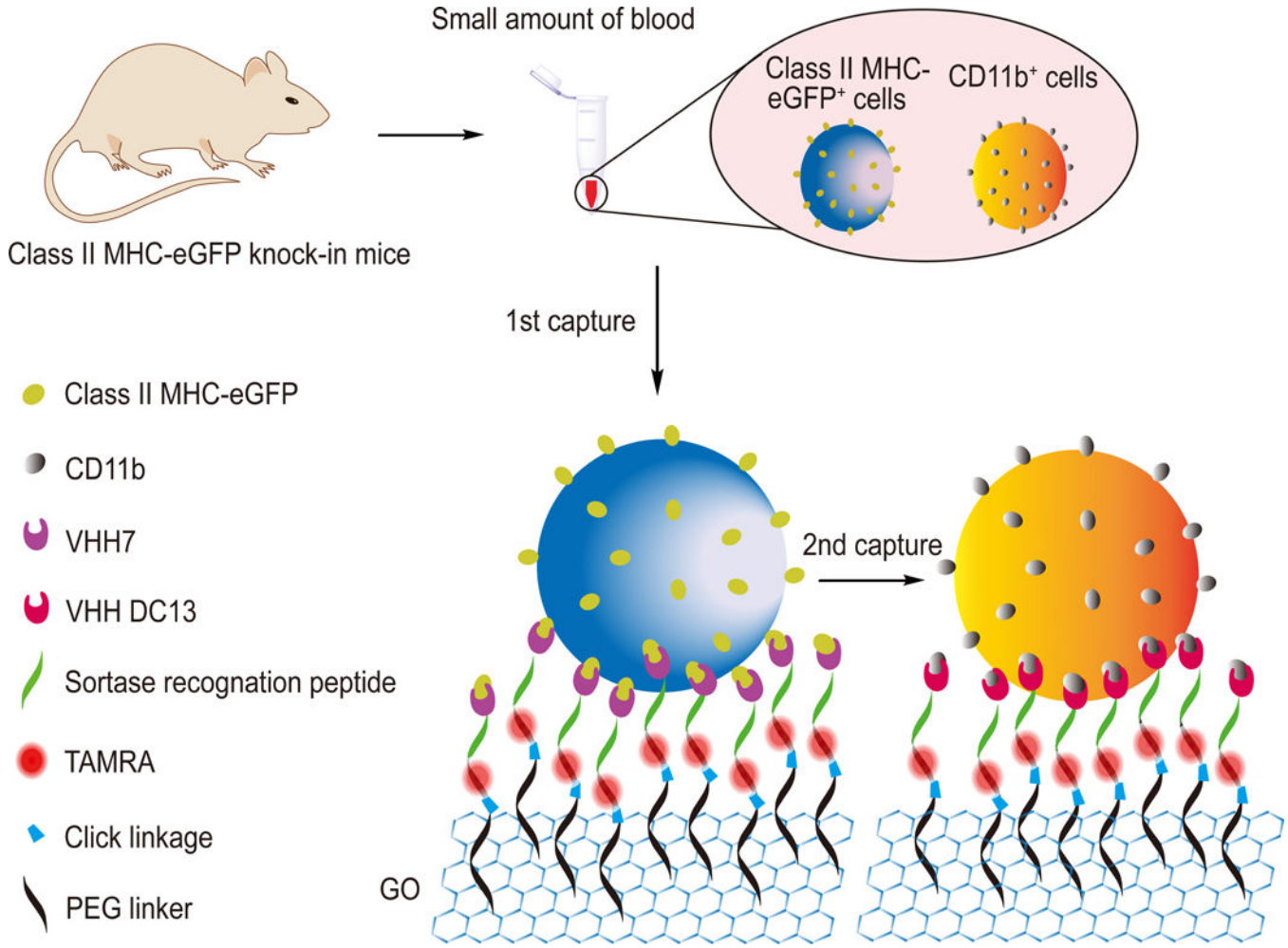

Figure 1.
Schematic illustration of VHH7 and VHH DC13-based GO substrates for capture of Class II MHC-eGFP$^+$ and CD11b$^+$ cells from whole blood.

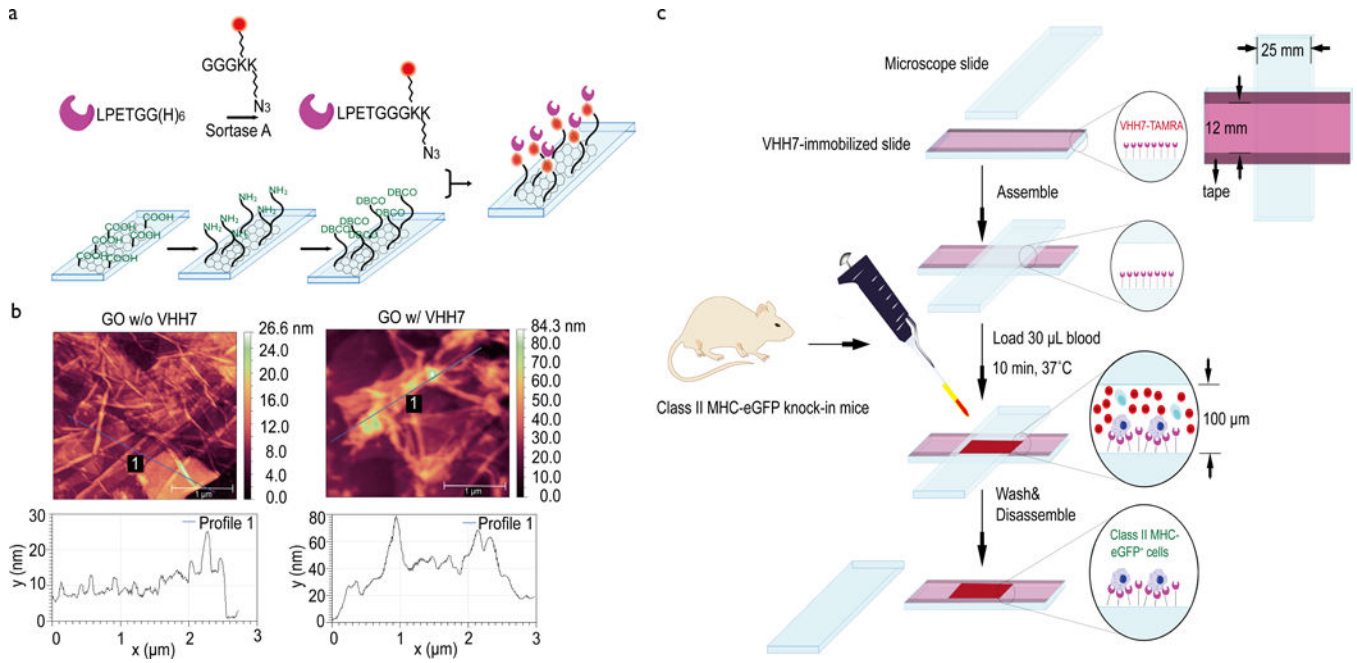

Figure 2.

Uniform attachment and characterization of a murine Class II MHC-specific targeting nanobody, VHH7, on GO nanosheets. a, Overview of sortase-mediated site-specific ligation of VHH7 onto GO nanosheets. VHH7 was C-terminally modified via a sortase-mediated ligation to install a TAMRA fluorophore and an azide. The GO nanosheet was functionalized with a DBCO handle for a “click” reaction with the azide-modified VHH7. b, AFM images of GO nanosheets and GO nanosheets with VHH7 immobilized on silicon substrates. The height difference between GO nanosheets with or without VHH7 immobilization was ~20–80 nm. The topography of the slide observed under the AFM is characteristic of protein bound to GO.[6] c, Whole blood analysis from Class II MHC-eGFP knock-in mice. A small volume of blood (30 μL) was loaded into the assembled chamber and incubated at 37°C for 10 min. The chamber was then disassembled and the cell-bearing substrate slide was gently washed 3x with PBS. After washing, cells were analyzed by fluorescence microscopy and quantitative image analysis.

Author Manuscript Author Manuscript Author Manuscript Author Manuscript

Author Manuscript Author Manuscript Author Manuscript Author Manuscript

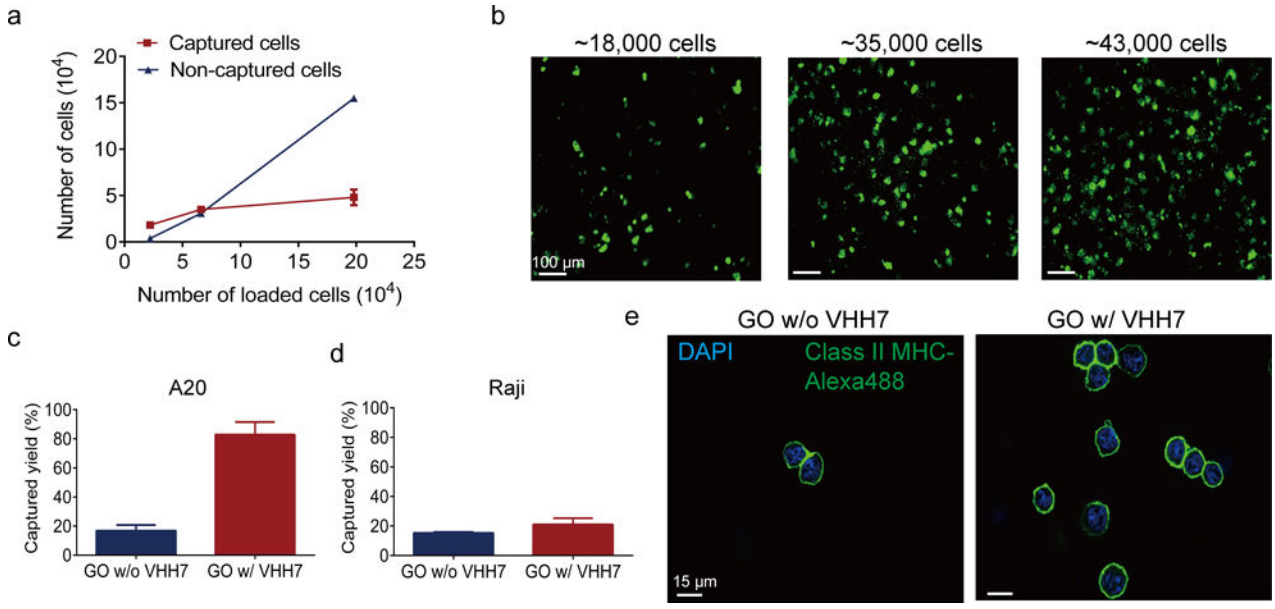

Figure 3.

Quantification and characterization of captured cells. a, Quantification of bound cells at different cell loading numbers. b, Microscopic observation of bound Class II MHC$^+$ cells. c, Quantification of captured A20 cells (murine Class II MHC$^+$) on substrates with and without VHH7 immobilization. d, Capture of Raji cells (murine Class II MHC-negative). e, Immunofluorescence images of captured A20 cells stained with Alexa488-labeled anti-Class II MHC and DAPI.

Author Manuscript Author Manuscript Author Manuscript Author Manuscript

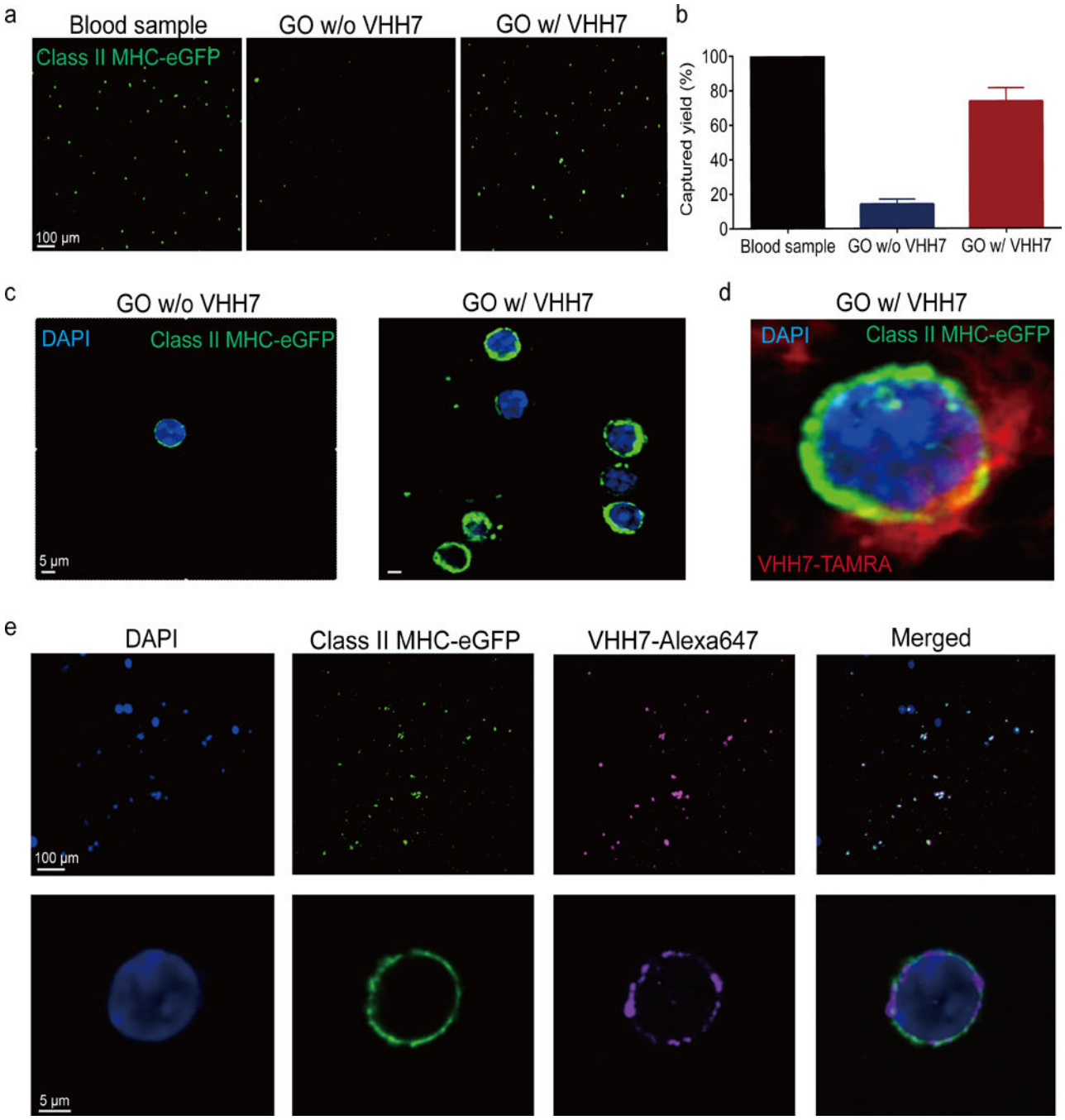

Figure 4.

Quantification and characterization of Class II MHC-eGFP^{+} cells from 30 μL of whole blood. a, Fluorescence microscopy of cells captured on VHH7-modified and unmodified GO substrates. b, Quantification of captured cells. c, Confocal microscopy of captured cells. d, Higher magnification of a captured cell, showing colocalization of the Class II MHC-eGFP signal with VHH7-TAMRA. e, Confocal microscopy images of VHH7-captured cells after staining with Alexa647-labeled VHH7.

Author Manuscript Author Manuscript Author Manuscript Author Manuscript

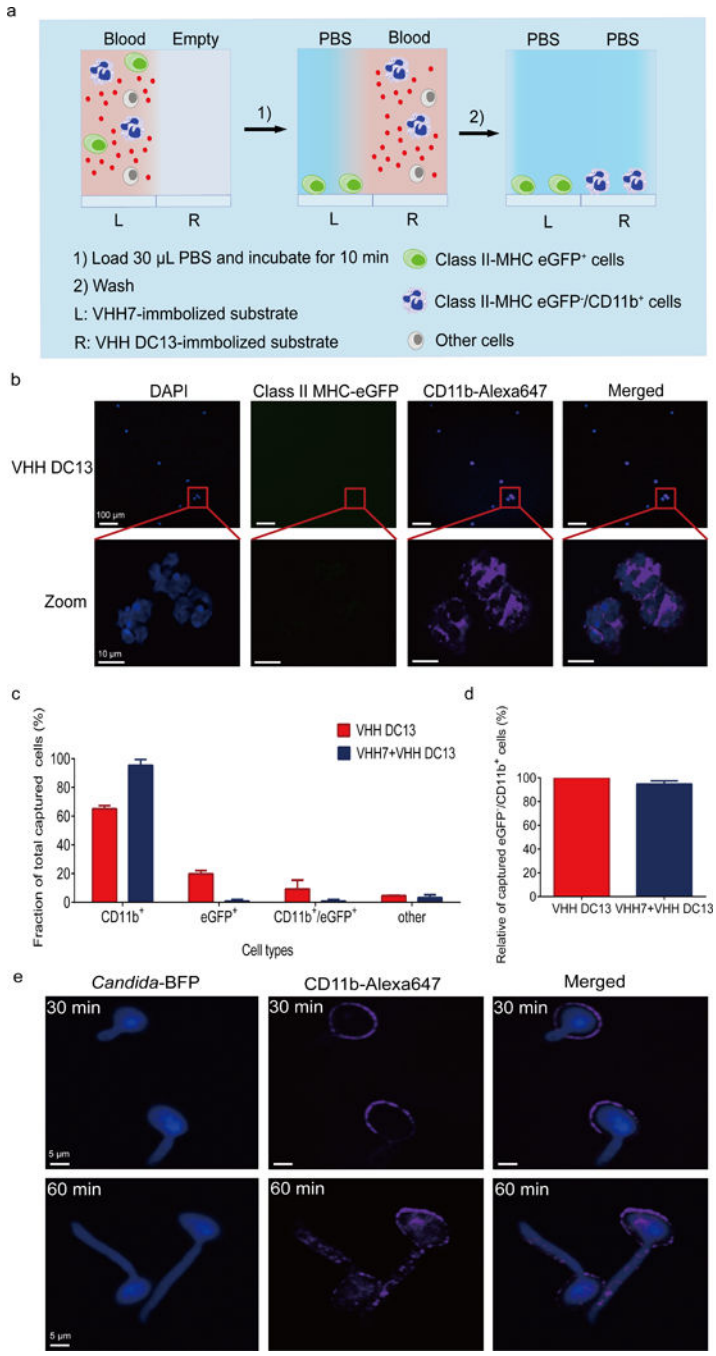

Figure 5.

Quantification and characterization of captured CD11b$^+$ cells by combined VHH7-VHH DC13-modified substrates. a, Cells were first passed over a VHH7 coated surface and captured subsequently on VHH DC13-modified substrates. b, Characterization of captured cells. c, Fraction of captured cells. d, Comparison of the yield of CD11b$^+$/eGFP$^-$ cells captured on a single (VHH DC13 alone) or dually modified VHH7-VHH DC13 substrate. e, Confocal microscopy of captured cells engaged in phagocytosis of *Candida albicans*.

Author Manuscript Author Manuscript Author Manuscript Author Manuscript

Captured cells were stained with Alexa647-labeled anti-CD11b antibody while *Candida albicans* expressed blue fluorescent protein to facilitate their detection.